Cracking of limestone calcined clay blended concrete and mortar under restrained shrinkage

Sumaiya Afroz [a], Quang Dieu Nguyen [b], Yingda Zhang [a], Taehwan Kim [a,*], Arnaud Castel [b]

[a] *School of Civil and Environmental Engineering, University of New South Wales, Sydney, NSW 2052, Australia*
[b] *School of Civil and Environmental Engineering, University of Technology Sydney (UTS), Sydney, NSW 2007, Australia*

ARTICLE INFO

ABSTRACT

This work is investigating restrained shrinkage induced early age cracking of limestone calcined clay (LC) blended concrete and mortar. A series of ring tests was conducted on LC blended concretes with 44% replacement of General Purpose (GP) cement and reference GP cement-only concretes. In addition, autogenous shrinkage and total shrinkage of concretes, mortars, and pastes were monitored to investigate the effect of the addition of LC on the different shrinkages and subsequent restrained shrinkage induced cracking. Results showed that LC blended concrete cracked earlier than the control mixes due to a high stress rate which is a function of the shrinkage of the restrained concrete ring. However, the autogenous shrinkage of concrete, rather than the total shrinkage, significantly influenced the early age cracking of LC blends. The ratio (total/autogenous) of shrinkage rates was proportional to the time to cracking for all mixes. The dependency of cracking on early-age autogenous shrinkage was further corroborated by the ring test results using LC blended mortar mixes considering various replacement levels ranging from 14% to 59%. Less early-age autogenous shrinkage in the LC blend with 59% replacement contributed to delayed cracking compared to other mortar mixes.

1. Introduction

Global warming and subsequent climate change are leading mankind towards a grave future. In the words of Pierrehumbert [1], "Let's get this on the table right away, without mincing words. With regard to the climate crisis, yes, it's time to panic". As a part of the global effort, the Paris Agreement was signed by 196 countries in 2015 agreeing to restrict the global temperature increase under 2 °C at the United Nations Framework Convention on Climate Change (COP 21). To achieve the goal stated in the Paris Agreement, the CO_2 emission must be reduced by 50%-80% before 2050 [2]. However, this task is daunting as the rate of increase in CO_2 emission has increased rapidly in recent times. In 2019 the CO_2 concentration in the atmosphere rose to 410 ppm compared to 285 ppm in 1850. The current rate of CO_2 emission can cause a projected temperature to rise about 5.8 °C by 2100 [3].

Concrete industry contributes to CO_2 emission and most of the emission is generated during the production of cement [4]. Cement production causes 5–8% anthropogenic CO_2 emissions and 90% of industrial CO_2 emissions [5–9]. To reduce the carbon footprint of concrete production, partial replacement of Portland Cement (PC) with Supplementary Cementitious Materials (SCMs) can be one of the most effective ways considering current availability and suitability for widespread adoption in the concreting industry to scale down the carbon emission and defeat global warming. In addition, partial cement replacement with SCMs has proven effective in improving the concrete durability [10].

Free shrinkage of concrete, which is an inherent property of concrete, has less impact on durability if concrete has no restraints. However, a concrete element under restrained shrinkage can develop cracks which not only impact the mechanical properties but also can act as a pathway for chemical ingression. Early age cracking in concrete can occur due to volumetric changes even before the service load is applied. Shrinkage-induced cracks under restraint may not lead to any structural damage immediately but can significantly affect the durability of a reinforced concrete structure. Unwanted and deleterious substances such as chlorides, sulphates and carbonates can penetrate through the cracks leading to severe deterioration as a result of cracks including corrosion of reinforcements, carbonation of concrete etc. [11,12].

Shrinkage can vary based on the property of the binders [13–16] influencing the tendency of early-age cracking [17–19]. Limestone calcined clay cement (LC) blend is a new option to replace Portland cement. This binder system has recently attracted global attention as a

---

Table 1
Chemical compositions of binders.

chemical composition	contents %		
	GP cement	calcined clay	limestone
silicon dioxide, SiO_2	18.96	51.22	1.10
aluminium oxide, Al_2O_3	4.81	39.37	0.24
ferric oxide, Fe_2O_3	3.14	2.56	0.17
calcium oxide, CaO	63.76	0.18	54.84
magnesium, MgO	1.20	0.10	1.53
sulfur trioxide, SO_3	2.37	0.02	0.03
sodium oxide, Na_2O	0.21	0.20	0.04
phosphorus pentoxide, P_2O_5	0.08	0.08	<0.01
potassium oxide, K_2O	0.46	0.09	0.01
titanium dioxide, TiO_2	0.22	2.88	<0.01
loss on ignition	3.96	2.19	43.11

potential low-carbon binder and it has been studied primarily for its mechanical properties [20]. Either calcined clay or limestone can be used to replace cement in a binary blend, and each reacts uniquely in the cementitious environment. Similar to a pozzolan, the reactive calcined kaolinite in calcined clay reacts with calcium hydroxide to produce C-A-S-H, aluminate hydrates (AFm), ettringite and occasionally stratlingite [21–23]. The extent of aluminium incorporation in C-A-S-H increases with the increasing availability of calcined kaolinite content [24]. Limestone replacing cement content acts as a filler material [25,26]. Under favourable conditions, limestone reacts with C_3A present in cement and produces mono and hemi carboaluminates [27,28]. In addition, limestone can enhance cement hydration [29] because the excess of CO_3^{2-} is adsorbed on C-S-H and this release OH^- from C-S-H through ion exchange [30]. In a limestone calcined clay ternary blend, the excess alumina from calcined clay reacts with calcite (limestone) in presence of calcium hydroxide and amplifies the carboaluminate formation [31–33]. Simultaneously, clinker and calcined clay reactions benefit from the presence of limestone in the ternary blend [24,34]. Recent studies reported that limestone calcined clay blend (LC blend) is more efficient in terms of, sulfate resistance [35,36], pore structure refinement [24], and durability against chloride intrusion [10,37,38].

However, the shrinkage of LC blends and its subsequent effects are still under debate. Despite extensive research into the mechanical performance and durability of LC blended binders, both shrinkage and restrained shrinkage induced cracking of LC blended concrete and their effects on the structural component of LC blended concrete have not been fully understood. Shrinkage can be defined as chemical, autogenous and drying shrinkage. Though all types of shrinkage are related to the movement of water, chemical and autogenous shrinkage closely derive from the hydration process. Measurement of pure drying shrinkage due to loss of water from pores to the surrounding environment is challenging unlike the shrinkages directly related to the hydration process. The overall shrinkage containing all types of shrinkage can be termed "total shrinkage" which is easy to measure by monitoring the length change of an element. A simplified approach to estimate the drying shrinkage qualitatively is to consider the difference between total and autogenous shrinkage, which has been used in several studies [13,39–42]. However, this simplified approach has an inherent limitation of underestimating the autogenous shrinkage component in total shrinkage due to the lack of available water lost to air exposure [13]. Some studies reported similar drying [37] and autogenous [43] shrinkage in LC blend compared to ordinary Portland cement (OPC)-based binder for up to 28 days. Other studies showed increased autogenous shrinkage [44,45] and decreased drying shrinkage [46] in LC blends. To the best knowledge of the author, the cracking tendency due to restrained shrinkage for LC blends has not been studied. To promote the viability of the LC blended concrete, it is critical to address the effect of shrinkage on the cracking of LC blends.

Though there is no data available on the cracking of LC blends, ECC (Engineered Cementitious Composite) with LC blend has been studied

for its tensile stress resistance behaviour. Zhu et al. [47] reported that ECC with LC blend had a higher strain capacity compared to OPC-ECC. The LC3-ECC samples showed the formation of microcracking upon application of tensile stress [47] which seemed to influence the strain capacity of LC3-ECC. However, the microcracks in ECC with LC blends formed under stress were reported to have opposite characteristics in two different studies. While Zhang et al. [48] reported larger and largely spaced cracks in ECC with LC blend, Zhu et al. [47] reported smaller and densely positioned cracks compared to OPC-ECC. Metakaolin-based ECC also showed larger crack width [49]. Knowledge about ECC can provide some indication about the cracking behaviour of LC blends but, to incorporate LC blends as a viable construction material, further study is needed related to LC blended concrete cracking.

In this study, the cracking tendency of LC blends was investigated for the first time using the ring testing method. The cracking tendency and the shrinkage were analyzed together to identify the extent of the influence of shrinkage development on cracking. For LC blended concrete, 44% replacement of cement was considered.

2. Materials and mix design

2.1. Materials

This study was conducted on paste, mortar, and concrete which were prepared with the following binders, i) General Purpose (GP) cement complying with AS 3972 [50], ii) calcined clay, and iii) limestone. The calcined clay was readily available which has been used in a previous study by the authors [42]. The calcined kaolinite and amorphous content were approximately 47.5% and 84% respectively. The commercially available limestone under the name of Omyacarb was supplied by Omya Australia. The chemical compositions of the binders are outlined in Table 1. D50 values from the particle size distribution of cement, calcined clay and limestone were 19 μm, 10 μm and 10 μm respectively. Sydney sand (2.65 specific gravity; 3.50% water absorption) and basalt (10 mm nominal size, 2.80 specific gravity; 1.08% water absorption) were used as fine and coarse aggregate respectively.

2.2. Sample preparation

2.2.1. Concrete

Six concrete mixes were considered in this study (Table 2) which can be broadly divided into GP cement-only mixes (C1, C2 and C3) and limestone calcined clay cement (LC) blended mixes (B1, B2 and B3) where 44% GP cement content was replaced with limestone (14%) and calcined clay (30%). The GP cement used contains 6% calcium carbonate [16,42]. Therefore, 44% replacement of GP cement by calcined clay and limestone was interpreted as equivalent to 50% clinker content which is the most commonly used replacement ratio for limestone calcined clay cement (LC). Three levels of total binder contents were considered for C and B concrete mixes resulting in different ranges (from ~30 MPa to ~50 MPa) of compressive strengths at 28 days (Table 2).

The dry binders and aggregates in saturated surface dry (SSD) condition were mixed for 2 min before adding water. Following that, the water was added and mixed further for 5 min. To maintain an acceptable workability ranging from 50 mm to 80 mm slump, up to 0.15% superplasticizer (MasterGlenium SKY 8100; a polycarboxylic ether polymer) with respect to the total binder content was used. A dose of this level has a negligible effect on shrinkage development [13].

2.2.2. Mortar and paste

The mortar and paste were prepared according to ASTM C305 [51] to further investigate the effect of LC replacement levels on restrained-ring cracking, autogenous shrinkage and total shrinkage (the details of experimental methods can be found in Section 3). The mix designs for mortars and pastes are summarized in Table 3 and the replacement levels for calcined clay and limestone in mortar and paste included 14%,

Table 2
Mix proportions of concrete.

mix	mix proportions by weight (kg/m^3)							28 days compressive strength, MPa
	GP cement	calcined clay	lime-stone	binder	coarse aggre-gate	fine aggre-gate	water to binder	
C1	310	0	0	310	1059	866	0.56	30.7 ± 1.05
C2	360	0	0	360	1025	839	0.49	32.5 ± 1.26
C3	510	0	0	510	927	759	0.40	50.5 ± 0.11
B1	173.6	93	43.4	310	1046	856	0.56	31.0 ± 0.91
B2	201.6	108	50.4	360	1010	826.5	0.49	38.4 ± 1.43
B3	510	153	71.4	510	906	742	0.40	44.8 ± 1.83

Table 3
Mix design and compressive strength of mortar samples.

mixes	binders %		calcined clay: limestone	sand: binder	w/b
	GP cement	calcined clay + limestone			
14L(M)	86	14	2:1	1:1	0.4
44L(M)	56	44	2:1	1:1	0.4
59L(M)	41	59	2:1	1:1	0.4
14L(P)	86	14	2:1	–	0.4
44L(P)	56	44	2:1	–	0.4
59L(P)	41	59	2:1	–	0.4

44% and 59%.

3. Experimental methods

3.1. Compressive strength of concrete

Concrete cylinders (100 mm in diameter and 200 mm in height) were prepared according to the mix designs shown in Table 2. After casting the cylinders in mould, the moulds were covered with wet cloths and stored at the ambient temperature (23 ± 2 °C) for one day and then specimens were demoulded and cured in the water for 28 days at a controlled temperature (23 ± 2 °C). The compressive strength of each concrete mix was determined at 28 days on three specimens according to ASTM C39 [52].

3.2. Ring test

An identical procedure previously followed by the authors [17] was carried out for the ring test of concrete and mortar. Thus, in this paper, the ring test experiment is briefly summarized because the details of the testing procedure and the description can be found in the previous study

[17]. The restrained concrete ring had a 5 mm thick steel inner steel ring and the unrestrained companion concrete ring was without any steel restraint as shown in Fig. 1. Both concrete rings in restrained and unrestrained conditions had identical dimensions i.e., radius, thickness and height. For each ring test, at least three strain gauges were installed on the surface of the inner ring for the restrained-ring tests and the surface of the concrete for the unrestrained-ring tests.

The concrete rings, both restrained and unrestrained, were demoulded 24 h after casting and strain gages attached to the rings recorded the developed strain values. The rings were allowed to dry in a temperature (23 ± 2 °C) and humidity (50 ± 3%) controlled room with exposed surfaces of top, bottom and outer circumference. The temperature and humidity were selected according to Australian standard AS1012. 13 [53]. Two restrained and two unrestrained rings were prepared for each concrete mix and two restrained rings were prepared for each mortar mix.

3.3. Shrinkage tests

3.3.1. Total and autogenous shrinkage of concrete

The total shrinkage (defined in Section 1) and autogenous shrinkage of concrete were measured on prism samples (75 × 75 × 280 mm) with three replicates per mix. The length changes of the samples were monitored with a vertical comparator at pre-designated times after demolding at 24 h. All surfaces of the total shrinkage samples were exposed and dried in a temperature (23 ± 2 °C) and humidity (50 ± 3%) controlled room during the test duration, which was identical to the exposure condition of the ring test. The autogenous shrinkage samples were wrapped with adhesive aluminium foils to restrict moisture loss and kept in the same room maintaining a of temperature 23 ± 2 °C.

3.3.2. Total shrinkage of mortar

After mixing mortar according to ASTM C305 [51], the mortar was poured into prism molds (75 × 75 × 280 mm) with pre-attached studs on both sides. Three prisms were prepared for each mix. The prisms were
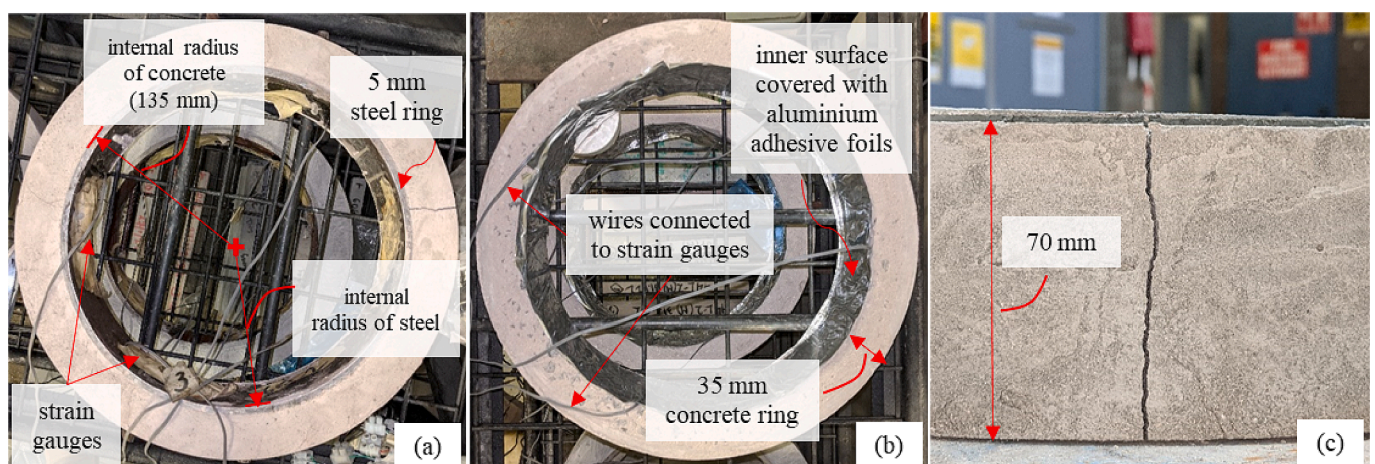
Fig. 1. Ring test setup of (a) restrained rings and (b) unrestrained rings, and (c) side view of a cracked restrained concrete ring.

demolded on day 1 and moved to the environmental chamber where temperature and humidity-controlled were controlled at 23 ± 2 °C and 50 ± 3% relative humidity, respectively according to Australian standard AS1012. 13 [53]. The initial length was recorded after demolding and subsequent readings were observed with a vertical length comparator.

3.3.3. Autogenous shrinkage of paste

The autogenous shrinkage of paste samples was determined on three replicates for each mix according to ASTM C1698 [54]. The freshly mixed paste was poured into the corrugated tubes ensuring there were no air bubbles and the ends were sealed by plugs. The paste specimens inside corrugated tubes were rotated at 4 rpm for 24 h to eliminate the effects of bleeding of water according to the recommendation by Mohr and Hood [55]. The specimens were kept at a constant temperature of 23 °C. The measurements started at the final setting and subsequent frequent measurements were recorded by a horizontal dilatometer as required. Prior to autogenous shrinkage testing, the final setting time of paste mixes was determined by calorimetry according to a technique by Hu et al. [56]. According to Hu et al. [56], the initial and final set times can be obtained from the first derivative of the heat evolution curves of the calorimetry test results. The final setting time was considered when the first derivative of the heat evolution curve reached zero. The final setting times of 20L(P), 50L(P) and 65L(P) were 470 min, 602 min and 418 min respectively.

4. Results and discussion

4.1. Concrete cracking and shrinkages

The ring test was conducted on three LC blended concrete with 44% replacement level but three different binder contents. As two replicate restrained rings were tested for each case, the first occurrence of cracking was considered for cracking time estimation, opting for a conservative approach similar to a previous work by the authors [17]. Therefore, the time to cracking and the strain values of the restrained ring were obtained from the ring that cracked first. In the case of the unrestrained ring, the average of the two replicates was taken to describe the strain values.

4.1.1. Concrete cracking

The ring test results of the LC blended concrete mixes are illustrated in Fig. 2. The data for the corresponding reference samples were adapted

from a previous work by the authors [17] as reference points. The overall comparison between the LC blended concrete and the reference is presented in Fig. 3.

The steel strain (restrained strain) shown in Fig. 2a was obtained from the strain gauge attached to the inner steel ring under the assumption that the restrained strain of the inner surface of the concrete
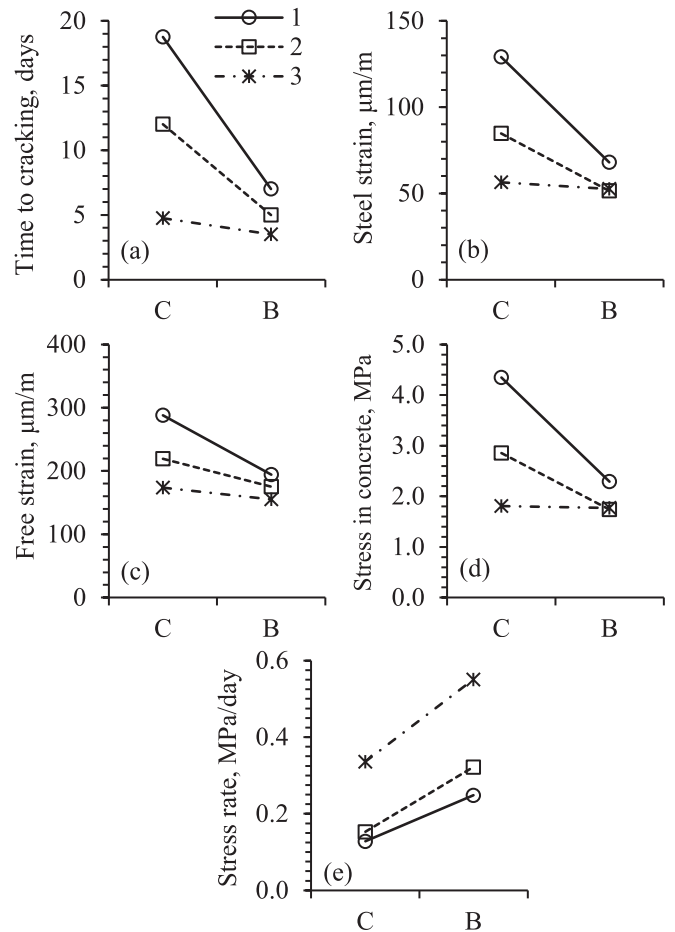

Fig. 3. Parameters related to cracking of concrete (a) time to cracking, (b) steel strain at cracking, (c) free strain at cracking, stress in concrete at cracking and (d) stress rate at cracking.
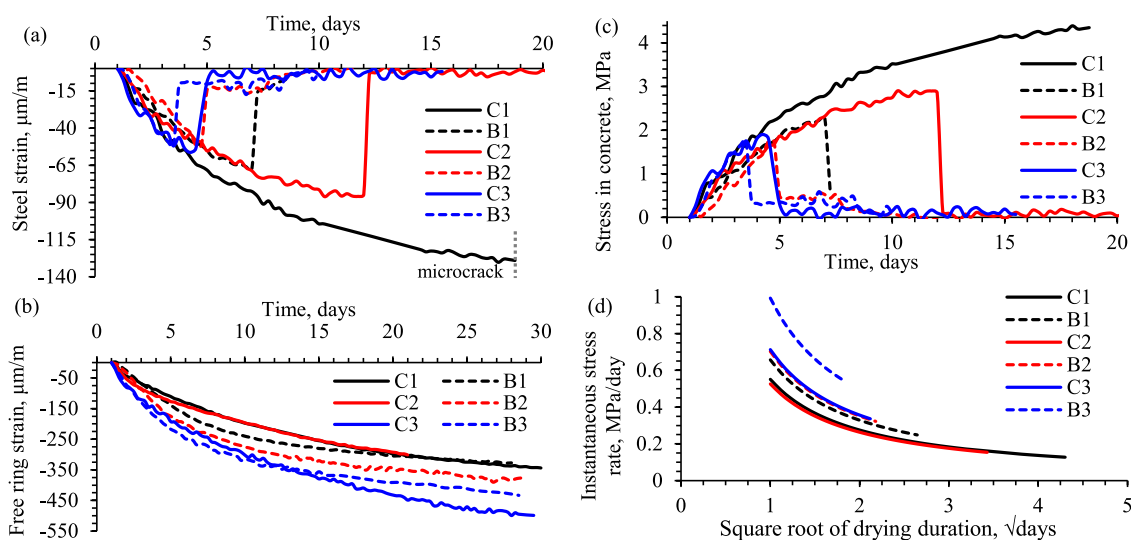

Fig. 2. Ring test results including (a) steel strain of restrained rings, (b) free strain of unrestrained rings, (c) stress in concrete of restrained rings and (d) instantaneous stress rate in restrained rings (data of C1, C2 and C3 adapted from [17] only for comparison).
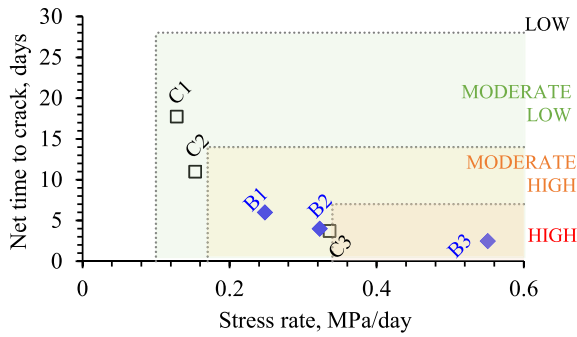
Fig. 4. Comparison of stress rates.

Fig. 6. Relation between the ratio of shrinkage rates and time to cracking.

ring is equal to the strain of the steel ring [17,57]. The sudden change/drop in steel strain indicated the stress release in the concrete ring due to cracking. All LC blends showed shorter times to cracking than those of the corresponding GP cement-based concrete. In other words, with the same grade of strength (the same w/b and total binder content) in concrete, the LC blended concrete cracked earlier than the GP cement-based concrete. In addition, increasing the compressive strength of concrete led to a decrease in cracking time for both blended and GP cement-based concretes (Fig. 2a). The steel strains at cracking observed in the restrained rings were also smaller for B2 and B3 than that for B1. The free strains observed in the companion unrestrained rings were progressively higher with the increasing strength of the concrete (Fig. 2b). The steel strain from the restrained ring can be converted into the stress in concrete by Eq. (1) [18,19] and the computed concrete stress is plotted in (Fig. 2c). B1 cracked at higher stress compared to the other two mixes, B2 and B3.

$$concrete\ stress,\ \sigma = -steel\ strain,\ \varepsilon_s * E_s * \frac{R_{OS}^2 - R_{IS}^2}{2R_{OS}^2} \frac{R_{OC}^2 + R_{OS}^2}{R_{OC}^2 - R_{OS}^2} \quad (1)$$

where E_s = elastic modulus of steel, R_{OS} = outer radius of the steel ring, R_{IS} = inner radius of the steel ring and R_{OC} = outer radius of the concrete ring.
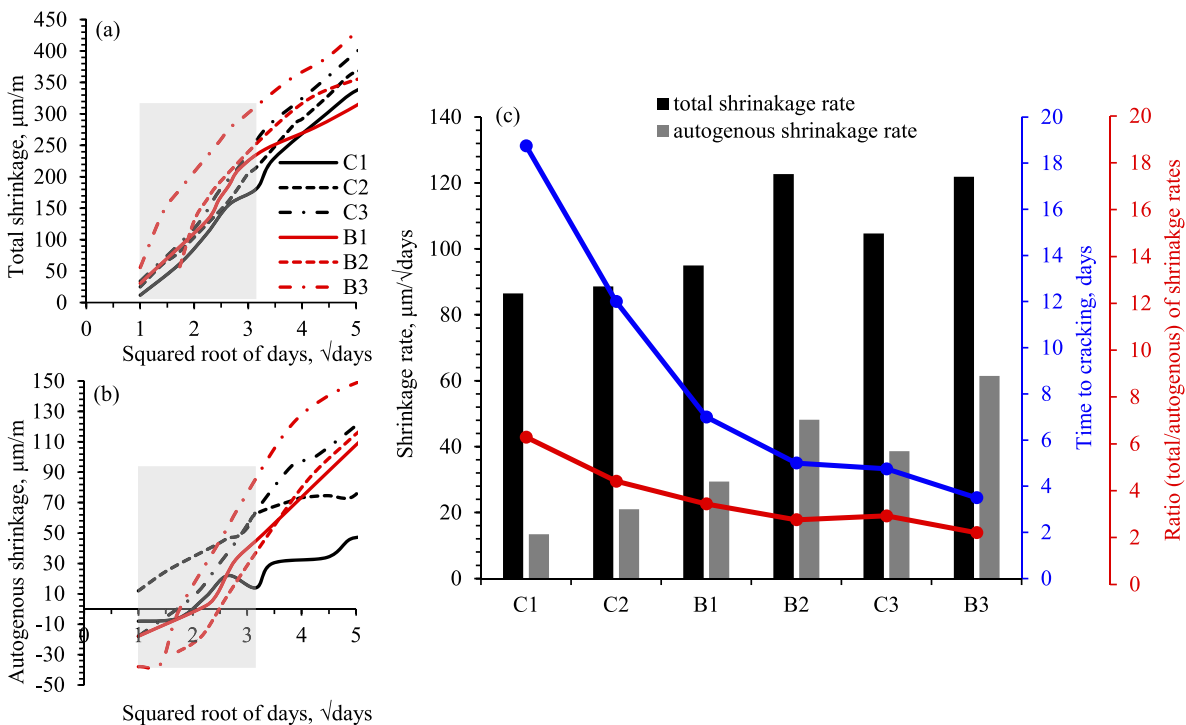
As concluded by Afroz et al. [17], the cracking tendency depends largely on the rate of stress (or strain) rather than the magnitude. The stress rate of the LC blends from the ring test was calculated by the method described in ASTM C1581 [58] and See et al. [59]. The stress rate (S) was derived from the steel strain using the following Eq. (2), where G ($=E_s R_{IC} h_s / R_{IS} h_c$) is a constant depending on the ring geometry [internal radius of concrete (R_{IC}) = 135 mm, internal radius of steel (R_{IS}) = 130 mm, the thickness of concrete (h_c) = 35 mm, thickness of steel (h_s) = 5 mm and steel elastic modulus (Es = 200 GPa)]. In this study, G was computed as 29.67 GPa. α is the strain rate factor in (m/m)/$\sqrt{day}$ obtained from steel strain data and t is the elapsed time.

$$stress\ rate,\ S = \frac{G|\alpha|}{2\sqrt{t}} \quad (2)$$

The resultant instantaneous stress rate is plotted in (Fig. 2d) against the corresponding drying duration. The drying duration was calculated from the moment the rings were exposed to air (at day 1). The stress rate at cracking was the highest for B3 and reduced progressively with the decreasing strength for B2 and B1.

The five different results (time to cracking, steel strain, free strain from unrestrained ring test, stress in concrete and stress rate) of the LC

Fig. 5. (a) total and (b) autogenous shrinkage of concrete prism specimens, (c) relationship between shrinkage rate and cracking.

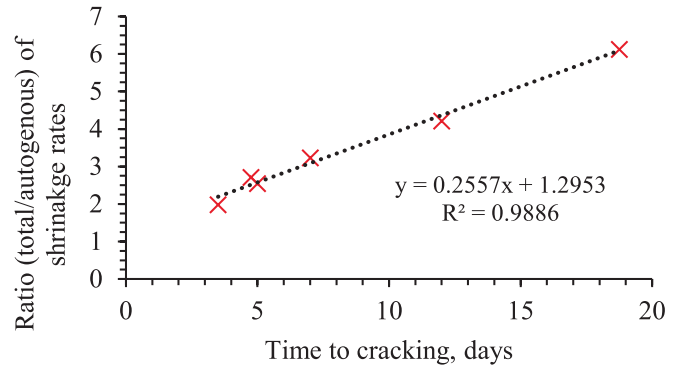blends at the time of cracking were compared with those obtained from the reference (GP cement-based concrete) in Fig. 3. The time to cracking was significantly lower in the LC blends compared to their counterpart cement only reference mixes (Fig. 3a). The time to cracking of B1, B2 and B3 were 7, 5 and 3.5 days respectively. B1, B2 and B3 cracked 62.67%, 58.33% and 26.32% earlier compared to C1, C2 and C3 respectively.

There is a clear impact of calcined clay and limestone addition on cracking time for the low strength concrete. However, for higher strength concrete, the cracking time has been less influenced by the calcined clay and limestone addition (see Fig. 3a). Although the cracking time was reduced by increasing the strength of LC blends (from 7 days for B1 to 3.5 days for B3), all of the LC blends cracked earlier than 7 days. On the other hand, the cracking time of reference concrete was reduced from 18.75 days for C1 to 4.75 days for C3 when increasing the strength. This indicates that the variation of compressive strength resulting from mix proportion within LC blends showed less impact on the cracking than the impact of strength on cracking time for corresponding reference samples.

The steel strain of the LC blends at the cracking time was also considerably lower than those from the reference mixes (see the case of C1 and B1 and C2 and B2 pairs in Fig. 3b). However, the steel strain at

cracking was similar for both C3 and B3. The free total shrinkage of the unrestrained rings at the time of cracking is shown in Fig. 3c. The range of the free shrinkage when cracks occurred in LC blends was quite narrow, between 155 μm/m to 194.5 μm/m. The stresses in concrete at cracking were also significantly smaller in LC blends compared to corresponding reference mixes except for high-strength concrete (C3 and B3) as shown in Fig. 3d. Though steel strain, free strain and stress in concrete at cracking were lower in the case of LC blends, the stress rate was higher compared to the reference mixes for all grades and possibly caused the earlier cracking (see Fig. 3e).

In the previous study by Afroz et al. [17], it was reported that the stress rate method can appropriately assess the cracking potentials of various concrete mixes including GP cement only, fly ash blends and slag blends. Fig. 4 presented the relationship between the time of cracking and the stress rate at the time of cracking. In the case of the LC blended concrete, all three mixes cracked before a net time to crack of 7 days. B3 fell within the "high potential for cracking" zone and the other two (B1 and B2) were categorized as "moderate-high potential for cracking" as specified in ASTM C1581 [58] (Fig. 4). It should be noted that corresponding reference samples showed less potential for cracking (C1 and C2 are in "moderate-low") and C3 is in "moderate-high").

The stress rate, S, is proportional to the steel strain rate as described in Eq. (2). Steel strain is the direct consequence of the shrinkage of the annular concrete ring around the inner steel ring. Therefore, the shrinkage rate in concrete can potentially provide an indication of the cracking tendency of any mix, which will be discussed further in the next section.

4.1.2. Free shrinkage of concrete and cracking

Shrinkage of concrete can be subdivided into autogenous shrinkage and drying shrinkage. Autogenous shrinkage occurs due to self-desiccation during the hydration process whereas drying shrinkage is
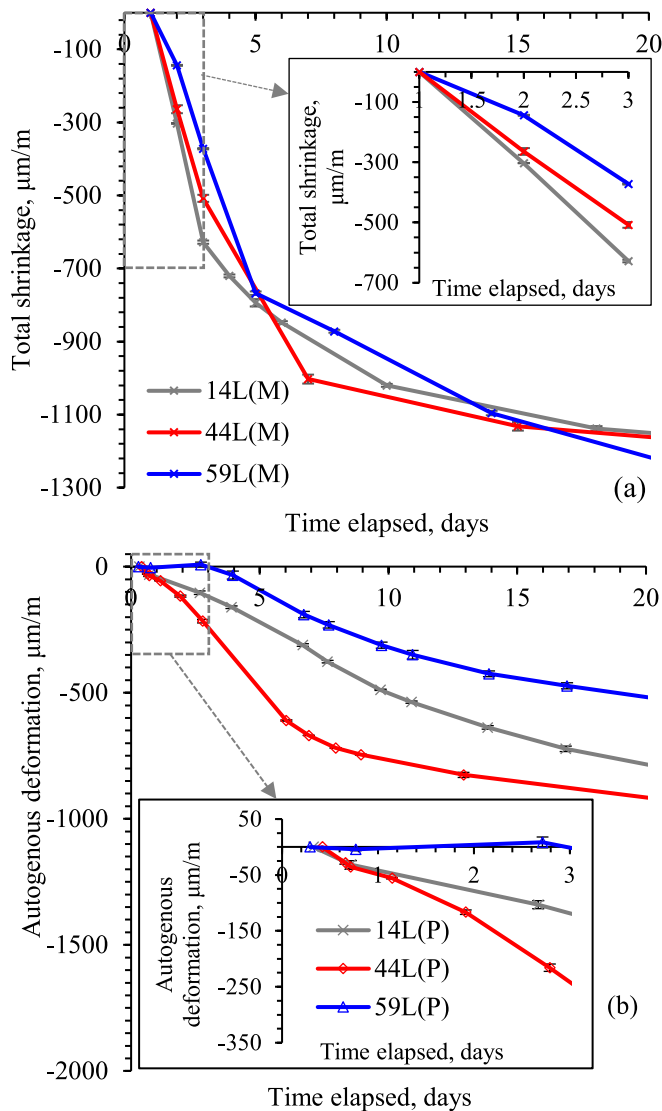

Fig. 7. (a) total shrinkage of LC blended mortars and (b) autogenous shrinkage of LC blended paste.
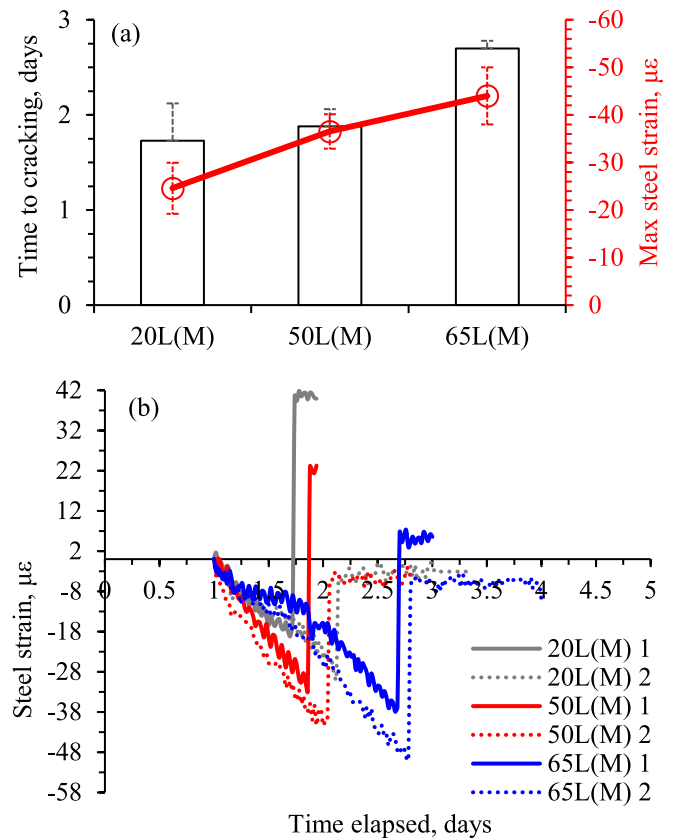

Fig. 8. Ring test results of LC blended mortar rings with varying replacement levels.

caused by the evaporation of water from the specimens. The sum of the autogenous and drying shrinkage can be termed total shrinkage [13]. Measuring pure drying shrinkage is difficult as the specimen subjected to air drying undergoes both autogenous and drying shrinkage. Otherwise, the measurement of autogenous shrinkage is possible by restricting the moisture exchange between the specimen and the environment. The ring specimens exposed to drying underwent both autogenous and drying shrinkage.

Though cracking is a direct consequence of restrained shrinkage, several previous studies found no clear relationship established between the magnitude of shrinkage and cracking [17,60,61]. This is because that shrinkage is not the sole factor to determine the cracking but other properties of concrete including the tensile strength, creep behaviour and elastic modulus also affect the time to cracking [62,63]. Hence arises the requirement of conducting the restrained ring test. Similar to the principal of stress rate calculation from the restrained ring test, the development rate of free shrinkage (based on the square root of elapsed time) can potentially indicate the extent of cracking tendency. To understand the effect of shrinkage rate on the cracking of rings, the total and autogenous shrinkage of prism specimens were plotted against the square root of elapsed time in Fig. 5a and 5b respectively. The slope of each line up to 10 days was defined as the shrinkage rate (the shaded part in Fig. 5a and 5b). The shrinkage values of the initial 10 days were considered to calculate the shrinkage rate as all LC blends cracked within 7 days indicating the early-age shrinkage development significantly impacted the cracking tendency. It is likely that the restrained stress causing the crack formation competed with the under-developed tensile strength during early ages determining the cracking tendency.

In Fig. 5c, the concrete mixes are ordered by the time to cracking (from the longest time to the shortest one), which revealed that a higher rate of autogenous shrinkage development was correlated with a shorter cracking time. The time to cracking and the ratio (total/autogenous) of shrinkage rates showed an identical trend. This trend is further illustrated in Fig. 6 and the time to cracking varied linearly with the ratio (total/autogenous) of shrinkage rates. As the ratio became smaller i.e., the autogenous shrinkage rate became higher, the time to crack was shorter. All three LC blends and C3 showed higher autogenous shrinkage rates and they cracked earlier (at days equal to or below 7 days). Higher-strength concrete tends to show higher autogenous shrinkage due to a low water-to-binder ratio as in the case of C3 and this trend was also observed in previous studies [14,16]. The shrinkage rate ratios were calculated for three additional GP cement-only concrete mixes in Appendix A. This shrinkage rate ratio (total shrinkage rate/autogenous shrinkage rate) may be a possible parameter for assessing cracking potential although further research should be conducted to validate this LC blends with 44% cement replacement showed higher autogenous shrinkage and higher cracking tendency than those from the reference mixes. Yio et al. [64] reported that high autogenous shrinkage can cause severe microcracking. Unlike the drying shrinkage, as cracks are occurring near the exposed surfaces, the microcracks induced by autogenous shrinkage were found to be well distributed throughout the entire volume. These microcracks, formed due to high autogenous shrinkage, may explain the earlier cracking tendency in LC blends. It has also been reported that, under equal levels of strain caused by uniaxial tension tests, ECC blended with calcined clay and limestone developed more closely spaced microcracks, though finer, compared to ECC with OPC-based counterparts [47]. Therefore, more microcracks in number may form as a result of autogenous shrinkage in LC blends. Under restrained stress, these microcracks can further connect and accelerate crack propagation.

4.2. Shrinkages and cracking of mortars and pastes with variable replacement levels of LC

LC blended concretes with 44% replacement level showed shorter cracking times compared to reference concretes due to higher

autogenous shrinkage rates. Afroz et al. [42] reported a high early age autogenous shrinkage in LC blended mixes due to an accelerated early-age hydration (up to 14 days) in presence of calcined clay. Dixit et al. [65] also found a higher degree of hydration in limestone-calcined clay mixes compared to OPC. Moreover, the presence of calcined clay, which is pozzolanic in nature, promotes pore refinement [65,66] which can contribute to a higher autogenous shrinkage compared to OPC system by increasing self-desiccation induced shrinkage [16]. In a previous study [67], the authors found that the autogenous shrinkage of LC blends was significantly dependent on the replacement levels which can influence the cracking tendency. Therefore, the effects of the replacement level on cracking were investigated using the mortar in this section.

4.2.1. Shrinkage of mortar and paste

The total shrinkage values of mortar specimens with varying LC replacement levels during early ages were similar (Fig. 7a). However, the initial shrinkage development (up to 3 days corresponding to the time to cracking of all mortar mixes) was slightly faster for 14L(M) and 44L(M) compared to 59L(M) (see inset of Fig. 7a). The slow development of total shrinkage in 59L(M) seemed to be the result of the slow development of the autogenous shrinkage of the paste component. Up to 3 days, 59L(P) showed negligible autogenous shrinkage of paste followed by 14L(P) and 44L(P) (see inset of Fig. 7b).

Though the total shrinkage development rates were similar for all calcined clay and limestone replacement levels, the different rates of autogenous shrinkage can result in varying cracking tendencies with respect to the replacement levels and will be explored in Section 4.2.2.

4.2.2. Mortar cracking

The mortar rings with 14%, 44% and 59% calcined clay and limestone cracked earlier than 3 days (Fig. 8a). The cracking of LC blended mortar rings was faster than the corresponding reference mortar mix which cracked at 3.09 days (from a previous study by the authors [17]). The first crack formation was at 1.73, 1.88 and 2.7 days for 14L(M), 44L(M) and 59L(M) respectively (Fig. 8a). The time to cracking was reported for the first crack formation between replicate rings opting for a conservative approach.

The longest time to cracking was for 59L(M) mix which also showed the highest steel strain at cracking. The effect of the slow development of the autogenous deformation (Fig. 7b) was also indirectly supported by the slow increase of steel strain in 59L(M) mix between 1 day to about 1.75 days (Fig. 8b).
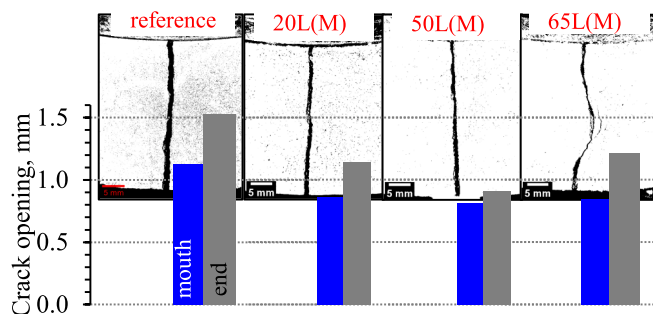

Fig. 9. Cracked restrained mortar rings and crack openings mortar mixes.

Table A1
Mix proportion of GP cement-only concrete mixes.

mix	mix proportions by weight (kg/m³)			
	GP cement	coarse aggregate	fine aggregate	water to binder
C4	450	966	790	0.43
C5	585	908	743	0.28
C6	650	880	720	0.22

As discussed in Section 4.1.2, the autogenous shrinkage exhibited a significant influence on LC blended mortar cracking. The high autogenous shrinkage at early ages seemed to be the main reason causing early cracking. Similar to shrinkage, the cracking tendencies of LC blends also considerably depend on calcined clay and limestone replacement levels.

The crack patterns of the mortar rings showed that the crack openings at the mouth (near the inner steel) and at the ends were similar for all three LC blends (Fig. 9) and the widths of the crack opening for LC blends were lower than that of the reference mix (GP cement only). The crack patterns were similar to a previous study [47] on LC blended ECC which reported tighter crack width compared to the OPC system.

5. Conclusions

This paper investigated the cracking tendency of limestone calcined clay (LC) cement blends, which is critical to promote the viability of using the LC blended concrete in structural components. The ring tests were conducted for mortar and concrete. Initially, the cracking behaviour of 44% LC blended concrete was compared with that of reference (GP cement only) mixes. In addition, the ring tests of LC blended mortar with different replacement levels (14%, 44% and 59%) were carried out to investigate the effect of calcined clay and limestone replacement rate on the cracking behaviour. Only one type of calcined clay with high reactivity has been used in these cracking-related investigations. The performance against restrained shrinkage-induced cracking might be different for other calcined clays, particularly with lower reactivity.

LC blended concrete with 44% replacement level cracked earlier compared to the reference concrete mixes for all mix proportions. Unlike reference mixes, the effect of strength on the cracking of LC blended concrete was insignificant. The stress rate exhibited a considerable effect on the early cracking of LC blends.

The stress rate in restrained rings can be considered as a function of the shrinkage development rate and the high autogenous shrinkage rate in LC blended concrete compared to reference mixes inducing the early age cracking. In addition, this study showed that the early-age shrinkage rate ratio (total shrinkage rate/autogenous shrinkage rate) was proportional to the time to cracking for all mixes. This ratio (total/autogenous) of shrinkage rates may be a possible parameter for assessing cracking potential although further research should be conducted to validate this assumption.

Similar to the concrete mixes, the autogenous shrinkage rate also influenced the cracking tendencies of the restrained rings using mortar mixes with varying calcined clay and limestone replacement levels. Mortar mixes with 59% calcined clay and limestone showed delayed cracking compared to 14% and 44% replacement levels due to the slow development of autogenous shrinkage.
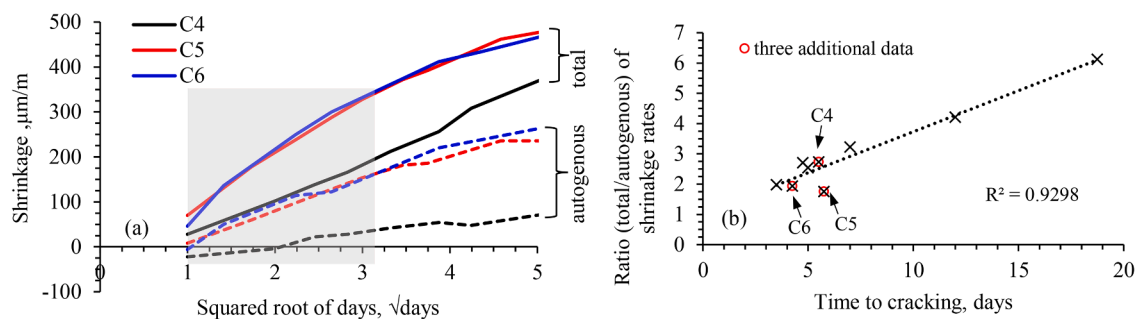
CRediT authorship contribution statement

Sumaiya Afroz: Conceptualization, Methodology, Validation, Formal analysis, Investigation, Data curation, Writing – original draft, Visualization. **Quang Dieu Nguyen:** Formal analysis, Investigation, Writing – review & editing. **Yingda Zhang:** Formal analysis, Investigation, Writing – review & editing. **Taehwan Kim:** Conceptualization, Methodology, Validation, Formal analysis, Resources, Writing – review & editing, Supervision. **Arnaud Castel:** Conceptualization, Methodology, Validation, Resources, Writing – review & editing, Supervision, Project administration, Funding acquisition.

Declaration of Competing Interest

The authors declare that they have no known competing financial interests or personal relationships that could have appeared to influence the work reported in this paper.

Data availability

Data will be made available on request.

Appendix A:. Additional data on total to autogenous shrinkage rate ratio

The shrinkage rates ratios (for shrinkage values up to 10 days) were calculated for three additional GP cement-only mixes. The mix proportions of the concrete mixes are presented in Table A1. Total and autogenous shrinkage development rates were steeper for C5 and C6 compared to C4 (Fig. A1a). The corresponding time to cracking from the ring test was adapted from a previous work by the authors [17] and the calculated shrinkage rate ratios (total shrinkage rate/autogenous shrinkage rate) were proportional to the time to cracking (Fig. A1b).

Fig. A1. Relation between the ratio of shrinkage rates and time to cracking with three additional data.

References

[1] R. Pierrehumbert, There is no Plan B for dealing with the climate crisis, Bull. At. Sci. 75 (5) (2019) 215–221.

[2] V.S. Sikarwar, A. Reichert, M. Jeremias, V. Manovic, COVID-19 pandemic and global carbon dioxide emissions: A first assessment, Sci. Total Environ. 794 (2021) 148770.

[3] E. Benhelal, E. Shamsaei, M.I. Rashid, Challenges against CO2 abatement strategies in cement industry: A review, J. Environ. Sci. 104 (2021) 84–101.

[4] C.-Y. Zhang, R. Han, B. Yu, Y.-M. Wei, Accounting process-related CO2 emissions from global cement production under Shared Socioeconomic Pathways, J. Clean. Prod. 184 (2018) 451–465.

[5] C. Chen, G. Habert, Y. Bouzidi, A. Jullien, Environmental impact of cement production: detail of the different processes and cement plant variability evaluation, J. Clean. Prod. 18 (2010) 478–485.

[6] L. Barcelo, J. Kline, G. Walenta, E. Gartner, Cement and carbon emissions, Mater. Struct. 47 (6) (2014) 1055–1065.

[7] H. Mikulčić, J.J. Klemeš, M. Vujanović, K. Urbaniec, N. Duić, Reducing greenhouse gasses emissions by fostering the deployment of alternative raw materials and energy sources in the cleaner cement manufacturing process, J. Clean. Prod. 136 (2016) 119–132.

[8] P.J.M. Monteiro, S.A. Miller, A. Horvath, Towards sustainable concrete, Nat. Mater. 16 (7) (2017) 698–699.

[9] C. Herath, C. Gunasekara, D.W. Law, S. Setunge, Performance of high volume fly ash concrete incorporating additives: a systematic literature review, Constr. Build. Mater. 258 (2020) 120606.

[10] Q.D. Nguyen, S. Afroz, A. Castel, Influence of calcined clay reactivity on the mechanical properties and chloride diffusion resistance of limestone calcined clay cement (LC3) concrete, J. Mar. Sci. Eng. 8 (2020) 301.

[11] M. Kayondo, R. Combrinck, W.P. Boshoff, State-of-the-art review on plastic cracking of concrete, Constr. Build. Mater. 225 (2019) 886–899.

[12] M.B. Otieno, M.G. Alexander, H.-D. Beushausen, Corrosion in cracked and uncracked concrete–influence of crack width, concrete quality and crack reopening, Mag. Concr. Res. 62 (6) (2010) 393–404.

[13] Q.D. Nguyen, S. Afroz, Y. Zhang, T. Kim, W. Li, A. Castel, Autogenous and total shrinkage of limestone calcined clay cement (LC3) concretes, Constr. Build. Mater. 314 (2022), 125720.

[14] Y. Zhang, S. Afroz, Q.D. Nguyen, T. Kim, D. Nguyen, A. Castel, J. Nairn, R. I. Gilbert, Autogenous shrinkage of fly ash and ground granulated blast furnace slag concrete, Mag. Concr. Res. 1–13 (2022).

[15] E.-I. Tazawa, S. Miyazawa, Influence of cement and admixture on autogenous shrinkage of cement paste, Cem. Concr. Res. 25 (2) (1995) 281–287.

[16] S. Afroz, Y. Zhang, Q.D. Nguyen, T. Kim, A. Castel, Effect of limestone in General Purpose cement on autogenous shrinkage of high strength GGBFS concrete and pastes, Constr. Build. Mater. 327 (2022) 126949.

[17] S. Afroz, Q.D. Nguyen, Y. Zhang, T. Kim, A. Castel, Evaluation of cracking potential parameters for low to high grade concrete with fly ash or slag, Constr. Build. Mater. 350 (2022), 128891.

[18] Y. Zhang, S. Afroz, Q.D. Nguyen, T. Kim, J. Eisenträger, A. Castel, T. Xu, Analytical model predicting the concrete tensile stress development in the restrained shrinkage ring test, Constr. Build. Mater. 307 (2021), 124930.

[19] A.B. Hossain, J. Weiss, Assessing residual stress development and stress relaxation in restrained concrete ring specimens, Cem. Concr. Compos. 26 (5) (2004) 531–540.

[20] M. Sharma, S. Bishnoi, F. Martirena, K. Scrivener, Limestone calcined clay cement and concrete: A state-of-the-art review, Cem. Concr. Res. 149 (2021) 106564.

[21] K. Scrivener, F. Martirena, S. Bishnoi, S. Maity, Calcined clay limestone cements (LC3), Cem. Concr. Res. 114 (2018) 49–56.

[22] P.S. de Silva, F.P. Glasser, Hydration of cements based on metakaolin: thermochemistry, Adv. Cem. Res. 3 (12) (1990) 167–177.

[23] A. Tironi, M.A. Trezza, A.N. Scian, E.F. Irassar, Assessment of pozzolanic activity of different calcined clays, Cem. Concr. Compos. 37 (2013) 319–327.

[24] F. Avet, K. Scrivener, Investigation of the calcined kaolinite content on the hydration of Limestone Calcined Clay Cement (LC3), Cem. Concr. Res. 107 (2018) 124–135.

[25] G. Menéndez, V. Bonavetti, E.F. Irassar, Strength development of ternary blended cement with limestone filler and blast-furnace slag, Cem. Concr. Compos. 25 (1) (2003) 61–67.

[26] S. Adu-Amankwah, M. Zajac, C. Stabler, B. Lothenbach, L. Black, Influence of limestone on the hydration of ternary slag cements, Cem. Concr. Res. 100 (2017) 96–109.

[27] V.L. Bonavetti, V.F. Rahhal, E.F. Irassar, Studies on the carboaluminate formation in limestone filler-blended cements, Cem. Concr. Res. 31 (6) (2001) 853–859.

[28] B. Lothenbach, G. Le Saout, E. Gallucci, K. Scrivener, Influence of limestone on the hydration of Portland cements, Cem. Concr. Res. 38 (2008) 848–860, https://doi.org/10.1016/j.cemconres.2008.01.002.

[29] A. Schöler, B. Lothenbach, F. Winnefeld, M. Ben Haha, M. Zajac, H.-M. Ludwig, Early hydration of SCM-blended Portland cements: A pore solution and isothermal calorimetry study, Cem. Concr. Res. 93 (2017) 71–82.

[30] A. Kumar, T. Oey, G. Falzone, J. Huang, M. Bauchy, M. Balonis, N. Neithalath, J. Bullard, G. Sant, The filler effect: The influence of filler content and type on the hydration rate of tricalcium silicate, J. Am. Ceram. Soc. 100 (2017) 3316–3328.

[31] M. Antoni, J. Rossen, F. Martirena, K. Scrivener, Cement substitution by a combination of metakaolin and limestone, Cem. Concr. Res. 42 (12) (2012) 1579–1589.

[32] T. Matschei, B. Lothenbach, F.P. Glasser, The role of calcium carbonate in cement hydration, Cem. Concr. Res. 37 (4) (2007) 551–558.

[33] S.S. Berriel, A. Favier, E.R. Domínguez, I.R.S. Machado, U. Heierli, K. Scrivener, F. M. Hernández, G. Habert, Assessing the environmental and economic potential of Limestone Calcined Clay Cement in Cuba, J. Clean. Prod. 124 (2016) 361–369.

[34] F. Avet, R. Snellings, A.A. Diaz, M. Ben Haha, K. Scrivener, Development of a new rapid, relevant and reliable (R3) test method to evaluate the pozzolanic reactivity of calcined kaolinitic clays, Cem. Concr. Res. 85 (2016) 1–11.

[35] Z. Shi, S. Ferreiro, B. Lothenbach, M.R. Geiker, W. Kunther, J. Kaufmann, D. Herfort, J. Skibsted, Sulfate resistance of calcined clay–Limestone–Portland cements, Cem. Concr. Res. 116 (2019) 238–251.

[36] Y. Dhandapani, S. Joseph, S. Bishnoi, W. Kunther, F. Kanavaris, T. Kim, E. Irassar, A. Castel, F. Zunino, A. Machner, Durability performance of binary and ternary blended cementitious systems with calcined clay: a RILEM TC 282 CCL review, Mater. Struct. 55 (2022) 1–29.

[37] Y. Dhandapani, T. Sakthivel, M. Santhanam, R. Gettu, R.G. Pillai, Mechanical properties and durability performance of concretes with Limestone Calcined Clay Cement (LC3), Cem. Concr. Res. 107 (2018) 136–151.

[38] Q.D. Nguyen, M.S.H. Khan, A. Castel, Chloride diffusion in limestone flash calcined clay cement concrete, ACI Mater. J. 117 (2020) 165–175.

[39] R. Wendner, M.H. Hubler, Z.P. Bažant, Optimization method, choice of form and uncertainty quantification of model B4 using laboratory and multi-decade bridge databases, Mater. Struct. 48 (4) (2015) 771–796.

[40] EN 12390-16, Testing hardened concrete - Part 16: Determination of the shrinkage of concrete, Eur. Stand. (2019).

[41] AS 3600, Concrete structures, Stand. Aust. (2018).

[42] S. Afroz, Y. Zhang, Q.D. Nguyen, T. Kim, A. Castel, Shrinkage of blended cement concrete with fly ash or limestone calcined clay, Mater Struct 56 (1) (2023).

[43] J. Ston, A. Hilaire, K. Scrivener, Autogenous Shrinkage and Creep of Limestone and Calcined Clay Based Binders, in: Calcined Clays Sustain, Concr., Springer, 2018, pp. 447–454.

[44] H. Du, S. Dai Pang, High-performance concrete incorporating calcined kaolin clay and limestone as cement substitute, Constr. Build. Mater. 264 (2020), 120152.

[45] R. Hay, L. Li, K. Celik, Shrinkage, hydration, and strength development of limestone calcined clay cement (LC3) with different sulfation levels, Cem. Concr. Compos. 127 (2022), 104403.

[46] Q.D. Nguyen, M.S.H. Khan, A. Castel, Engineering properties of limestone calcined clay concrete, J. Adv. Concr. Technol. 16 (8) (2018) 343–357.

[47] H. Zhu, D. Zhang, T. Wang, H. Wu, V.C. Li, Mechanical and self-healing behavior of low carbon engineered cementitious composites reinforced with PP-fibers, Constr. Build. Mater. 259 (2020), 119805.

[48] D. Zhang, B. Jaworska, H. Zhu, K. Dahlquist, V.C. Li, Engineered Cementitious Composites (ECC) with limestone calcined clay cement (LC3), Cem. Concr. Compos. 114 (2020), 103766.

[49] E. Özbay, O. Karahan, M. Lachemi, K.M.A. Hossain, C. Duran Atiş, Investigation of properties of engineered cementitious composites incorporating high volumes of fly ash and metakaolin, ACI Mater. J. 109 (2012).

[50] AS 3972, General purpose and blended cements, Aust. Stand. (2010) 1–29.

[51] ASTM C305-20, Standard Practice for Mechanical Mixing of Hydraulic Cement Pastes and Mortars of Plastic Consistency, ASTM Int. West Conshohocken, PA. (2020).

[52] ASTM C39/C39M-21, Standard Test Method for Compressive Strength of Cylindrical Concrete Specimens, ASTM Int. West Conshohocken, PA. (2021).

[53] AS 1012.13:2015, Methods of testing concrete Determination of the drying shrinkage of concrete for samples prepared in the field or in the laboratory, Stand. Aust. (2015).

[54] ASTM C1698-19, Standard Test Method for Autogenous Strain of Cement Paste and Mortar, ASTM Int. West Conshohocken, PA. (2019).

[55] B.J. Mohr, K.L. Hood, Influence of bleed water reabsorption on cement paste autogenous deformation, Cem. Concr. Res. 40 (2) (2010) 220–225.

[56] J. Hu, Z. Ge, K. Wang, Influence of cement fineness and water-to-cement ratio on mortar early-age heat of hydration and set times, Constr. Build. Mater. 50 (2014) 657–663.

[57] W. Hansen, Report on early-age cracking, Concr. Int. 33 (2011) 48–51.

[58] ASTM C1581/C1581M-18a, Standard Test Method for Determining Age at Cracking and Induced Tensile Stress Characteristics of Mortar and Concrete under Restrained Shrinkage, ASTM Int. West Conshohocken, PA. (2018).

[59] H.T. See, E.K. Attiogbe, M.A. Miltenberger, Potential for restrained shrinkage cracking of concrete and mortar, Cem. Concr. Aggregates. 26 (2) (2004) 1–8.

[60] Y. Wei, W. Hansen, Early-age strain–stress relationship and cracking behavior of slag cement mixtures subject to constant uniaxial restraint, Constr. Build. Mater. 49 (2013) 635–642.

[61] S. Tongaroonsri, S. Tangtermsirikul, Effect of mineral admixtures and curing periods on shrinkage and cracking age under restrained condition, Constr. Build. Mater. 23 (2) (2009) 1050–1056.

[62] I. Khan, A. Castel, R.I. Gilbert, Tensile creep and early-age concrete cracking due to restrained shrinkage, Constr. Build. Mater. 149 (2017) 705–715.

[63] X. Hu, Z. Shi, C. Shi, Z. Wu, B. Tong, Z. Ou, G. De Schutter, Drying shrinkage and cracking resistance of concrete made with ternary cementitious components, Constr. Build. Mater. 149 (2017) 406–415.

[64] M.H.N. Yio, M.J. Mac, Y.X. Yeow, H.S. Wong, N.R. Buenfeld, Effect of autogenous shrinkage on microcracking and mass transport properties of concrete containing supplementary cementitious materials, Cem. Concr. Res. 150 (2021), 106611.

[65] A. Dixit, H. Du, J. Dang, S. Dai Pang, Quaternary blended limestone-calcined clay cement concrete incorporating fly ash, Cem. Concr. Compos. 123 (2021), 104174.

[66] J. Dang, J. Zhao, H. Du, S. Dai Pang, Calcined marine clay as cement replacement to make low-carbon mortar, ACI Mater. J. 119 (2022).

[67] S. Afroz, Y. Zhang, Q.D. Nguyen, T. Kim, A. Castel, Shrinkage of limestone calcined clay cement (LC3), in: Int. Conf. Calcined Clays Sustain. Concr., 2022.